

φ -State and Inverted Fraunhofer Pattern in Nonaligned Josephson Junctions

Mohammad Alidoust* and Jacob Linder†

Department of Physics, Norwegian University of Science and Technology, N-7491 Trondheim, Norway

(Dated: January 28, 2013)

A generic nonaligned Josephson junction in the presence of an external magnetic field is theoretically considered and an unusual flux-dependent current-phase relation (CPR) is revealed. We explain the origin of the anomalous CPR via the current density flow induced by the external field within a two-dimensional quasiclassical Keldysh-Usadel framework. In particular, it is demonstrated that nonaligned Josephson junctions can be utilized to obtain a ground-state other than 0 and π , corresponding to a so-called φ -junction, which is tunable via the external magnetic flux. Furthermore, we show that the standard Fraunhofer central peak of the critical supercurrent may be inverted into a local minimum solely due to geometrical factors in planar junctions. This yields good consistency with a recent experimental measurement displaying such type of puzzling feature [R. S. Keizer *et al.*, *Nature* **439**, 825 (2006)].

PACS numbers: 74.50.+r, 74.45.+c, 74.25.Ha, 74.78.Na

A sinusoidal current-phase relation (CPR) and Fraunhofer response of the critical supercurrent through a s -wave Josephson contact exposed to an external magnetic field are often considered to be standard characteristics of such junctions¹⁻⁴. Nevertheless, several theoretical studies have been dedicated to the aim of achieving an experimentally accessible situation where the CPR is non-sinusoidal⁶⁻⁸. In this case, the Josephson ground-state may be characterized by an arbitrary superconducting phase difference φ ^{6-8,21,23}, rather than the so-called 0- and π -states⁹. The first experimental realization of such a φ -junction was very recently reported in Ref. 14.

Recent studies have also pointed to the fact that the conventional Fraunhofer pattern in Josephson junctions may be modified by the junction geometry or interfacial pair breaking^{4,10,21}. The suppression of the central peak in the interference pattern can also occur in systems consisting of a superposition of multiple 0- π junctions^{8,10,21}. However, there still exists experimentally observed magnetic interference profiles that remain unsettled in terms of a theoretical explanation of the physical origin^{11,12}. In particular, Keizer *et al.*¹¹ observed an anomalous interference pattern with a local minimum at zero flux in addition to slowly damped oscillations of the critical supercurrent compared to the standard Fraunhofer pattern. The setup in Ref. 11 consisted of a planar Josephson junction where superconducting leads were deposited on a same side of a half-metallic ferromagnetic strip which was fully spin polarized. Figure 1 A) depicts diagrammatically the mentioned experimental setup. To study the system theoretically, Ref. 13 utilized the Eilenberger formalism in a ballistic planar junction, similar to the setup of Ref. 11, while neglecting the orbital motion²² of the quasiparticles. Consequently, an effective spatially dependent superconducting phase difference was obtained via Ginzburg-Landau theory and substituted into the Eilenberger equation. An almost Φ_0 -periodic pattern with non-zero minima of the critical current with respect to external magnetic flux were found due to the appearance of second harmonic ($\sin 2\varphi$, see also Ref. 6). However, the inverted interference pattern with a local minimum at zero flux was not reproduced.

In this Rapid Communication, we consider a generic class of Josephson junctions in the presence of an external magnetic

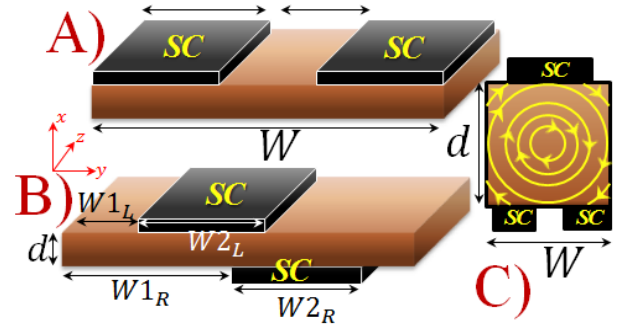


FIG. 1: Diagram of considered setups in this paper. An external magnetic field \mathbf{H} (not shown) is applied to the junction in the z direction. The junction lengths and widths are d and W , respectively. A): The planar Josephson junction that has experimentally been studied in *e.g.* Ref. 11. The widths of the superconducting leads are assumed to be W_{1L} and $W - (W_{1L} + W_{2L})$. B): The usual stacked geometry of a Josephson junction with displaced superconducting leads. The superconducting leads' sizes are W_{1L} and W_{2R} at the top and bottom of junction, respectively. C): Qualitative view of the current density flow inside the normal strip subject to an external magnetic field, which is used to describe the origin of the addressed unusual CPR.

field where the position of the superconducting leads relative each other is not necessarily aligned (see Fig. 1). The obtained results are derived *without recourse to any ansatz* - we have instead utilized a quasiclassical Keldysh-Usadel technique with the numerical approach in Ref. 10 and solved exactly the resultant linearized equations of motion for the Green's function. As our *first* main result, we unveil that the origin of the unexpected interference pattern in the experiment of Ref. 11 lies within the geometry of the setup. In this way, the absence of the standard Fraunhofer pattern, which has not been clearly understood, is resolved. In addition to this, we demonstrate as our *second* main result that the CPR in non-aligned junctions takes on a very unusual feature: it becomes shifted by a term proportional to the external flux Φ , namely $I(\varphi, \Phi) = I_0(\Phi) \sin(\varphi + \Theta(\Phi))$ where φ is the superconduct-

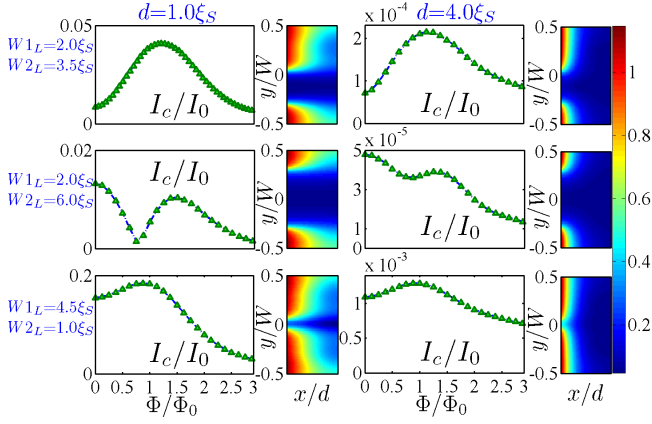


FIG. 2: Critical supercurrent as a function of external magnetic flux Φ through the normal part of junction. The corresponding pair potential spatial map is given with $\varphi = 0$. Throughout the paper we have assumed that the junction width is fixed at $W=10\xi_S$. The first and second columns show the critical current I_c/I_0 vs normalized external magnetic flux Φ/Φ_0 and the corresponding pair potential spatial maps with thicknesses $d=\xi_S$ and $4\xi_S$, respectively. Each row indicates different values of $W1_L$ and $W2_L$ namely, the first superconducting lead size and the separation of the superconducting leads, respectively (see Fig. 1).

ing phase difference and Θ is a geometry-dependent function. Our investigations reveal that the well-known sinusoidal supercurrent and consequently the Fraunhofer pattern manifest *only in a specific* situations. This result is explained in terms of the current density flow stemming from the orbital effect induced by the magnetic field. An interesting consequence of the external magnetic flux-shifted superconducting phase-difference is that the ground-state of the system may be tuned via the external field so that the equilibrium phase difference differs from the conventional 0 or π solutions making a so-called φ -junction. This might constitute a simpler alternative to realizing a φ -state compared to the array of SFS junctions considered in Ref. 14.

In the presence of impurity scattering, i.e. the diffusive regime of transport, the quasiparticles' momentum is integrated over all directions in the space which leads the Usadel equation. Solving the Usadel equation in the presence of a magnetic field allows one to compute the current density flow profile in the junction which is different from the individual trajectories taken by each quasiparticle. Grazing trajectories are not well-defined in this regime although they need to be considered carefully in the clean regime (where the Eilenberger equation is valid)²².

The starting point for the analysis is the equation of motion for the Green's function in the diffusive regime provided by the Usadel equation¹⁵:

$$D[\hat{\partial}, \check{G}(x, y, z)[\hat{\partial}, \check{G}(x, y, z)]] + i[\varepsilon\hat{\rho}_3, \check{G}(x, y, z)] = 0, \quad (1)$$

where $\hat{\rho}_3$ is 4×4 Pauli matrix. Here, ε is the particles' energy measured from the Fermi level and D is medium diffusive constant. In the presence of an external magnetic field \mathbf{H} and its vector potential \mathbf{A} , $\hat{\partial} \equiv \vec{\nabla}\hat{1} - ie\mathbf{A}(x, y, z)\hat{\rho}_3$ provided

that¹⁶

$$[\hat{\partial}, \hat{G}(x, y, z)] = \vec{\nabla}\hat{G}(x, y, z) - ie[\mathbf{A}(x, y, z)\hat{\rho}_3, \hat{G}(x, y, z)]. \quad (2)$$

The vector potential is an arbitrary quantity except for the restriction $\vec{\nabla} \times \mathbf{A} = \mathbf{H}$. We use the Coulomb gauge $\vec{\nabla} \cdot \mathbf{A} = 0$ throughout our calculations and assume that the external magnetic field is oriented in the z direction i.e. $\mathbf{H} = H\hat{z}$ (see Fig. 1). Thus, we may use $\mathbf{A} = -yH\hat{x}$. In general, the Usadel equation should be simultaneously solved along with the Maxwell equation $\vec{\nabla} \times \mathbf{H} = \mu_0\mathbf{j}$ in a self-consistent manner to take into account the influence of screening currents. The experimentally relevant scenario is considered where the width of the junction W is smaller than the Josephson penetration length λ_J , allowing us to ignore the screening of the magnetic field^{4,10,17}. The Usadel motion equation yields a system of nonlinear coupled complex partial differential equations that should be supported by suitable boundary conditions for studying junctions. In our Josephson system, we employ the Kupriyanov-Lukichev boundary conditions at N/S interfaces¹⁸ and control the leakage of superconductive correlations into the normal strip using an interface parameter ζ ;

$$\zeta(\hat{G}(x, y, z)\hat{\partial}\hat{G}(x, y, z)) \cdot \hat{\mathbf{n}} = [\hat{G}_{\text{BCS}}(\varphi), \hat{G}(x, y, z)], \quad (3)$$

in which $\hat{\mathbf{n}}$ is a unit vector denoting the perpendicular direction to an interface and φ is the bulk superconducting macroscopic phase. We define $\zeta = R_B/R_F$ as the ratio between the resistance of the barrier region and the resistance in the normal sandwiched strip. The bulk solution for the retarded Green's function in a s -wave superconductor is given by¹⁶ $g_{\text{BCS}}^R = \cosh \vartheta(\varepsilon)$ and $f_{\text{BCS}}^R = e^{i\varphi} \sinh \vartheta(\varepsilon)$ in which $\vartheta(\varepsilon) = \text{arctanh}(|\Delta|/|\varepsilon|)$. For a weak proximity effect ($\zeta \gg 1$), the normal and anomalous Green's functions can be approximated by $g^R \simeq 1$ and $|f^R| \ll 1$, respectively. The current density vector is expressed via the Keldysh block as

$$\mathbf{J}(\vec{R}, \varphi) = J_0 \int d\varepsilon \text{Tr}\{\rho_3(\hat{G}(x, y, z)[\hat{\partial}, \hat{G}(x, y, z)])^K\}. \quad (4)$$

Here, J_0 is a normalization constant proportional to the density of states N_0 at the Fermi level. The total supercurrent I is obtained by integrating the current density over the interface area of the superconducting banks. The flux penetrating the junction is given by $\Phi = dWH$. We also investigate the spatial variation of pair potential inside the normal region calculated via:

$$U = U_0 \text{Tr}\{(\hat{\rho}_1 - i\hat{\rho}_2) \int d\varepsilon \hat{\tau}_3 \check{G}^K(x, y, z)\}, \quad (5)$$

where $U_0 = -N_0\lambda/16$ ¹⁶. In the presence of an external magnetic field, the resultant differential equations and boundary conditions have a more complicated coordinate-dependence which renders an analytical solution virtually impossible. Without any orbital effect, such a solution may be obtained²³. To study the considered Josephson junction we use a collocation finite element numerical method the same as Ref. 10. The components of approximate solution are assumed to be

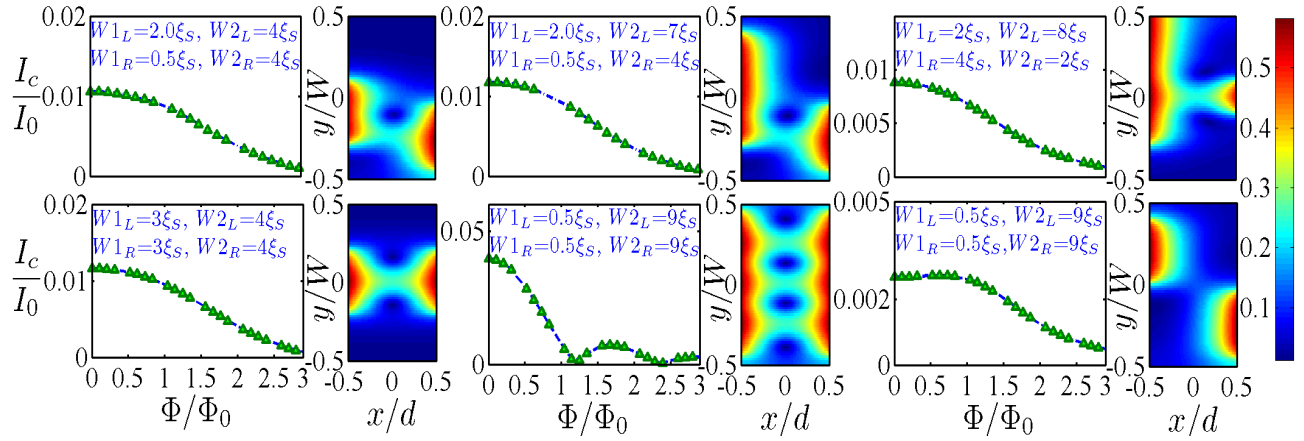


FIG. 3: Critical supercurrent against external magnetic flux and corresponding pair potential spatial maps of standard (stacked) Josephson junctions with displaced superconducting leads including various lead sizes. For the pair potential maps, the superconducting phase difference and external magnetic flux are fixed at $\varphi=0$ and $\Phi=4\Phi_0$, respectively. The junction thickness and width are set to $d=2\xi_S$ and $W=10\xi_S$, respectively.

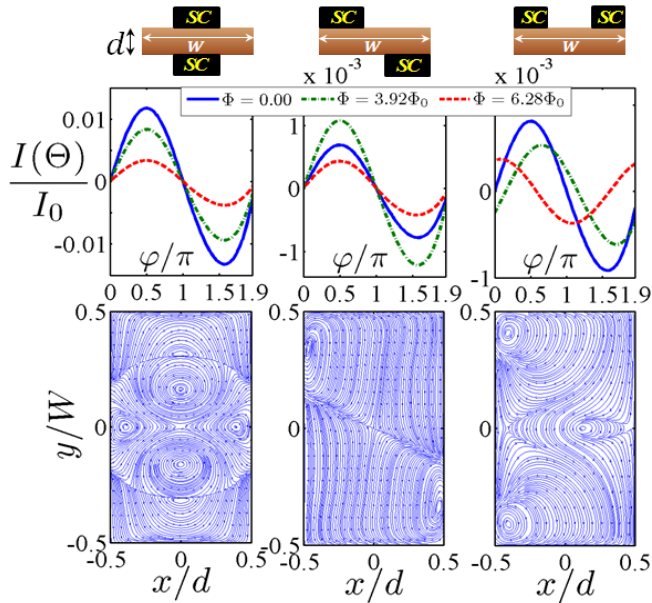


FIG. 4: i) Left column: $W1_L = 3\xi_S$, $W2_L = 4\xi_S$, $W1_R = 3\xi_S$, $W2_R = 4\xi_S$, ii) middle column: $W1_L = 6\xi_S$, $W2_L = 4\xi_S$, $W1_R = 0$, $W2_R = 4\xi_S$ and finally iii) right column: $W1_L = 2\xi_S$, $W2_L = 6\xi_S$. The top panels represent the CPRs for various values of $\Phi/\Phi_0=0, 3.92, 6.28$. The current density spatial maps in the bottom row show the results for $\varphi = 0$ and $\Phi = 4\Phi_0$. The superconducting leads' sizes are set equal to $4\xi_S$ for all cases as schematically depicted on top of each column.

linear combinations of bicubic Hermite basis functions satisfying the boundary conditions. Ultimately, the resultant non-symmetric linear algebraic equations are solved via a Jacobi conjugate-gradient method. For more details, see Ref. 19. All lengths and energies are normalized by the superconducting coherent length ξ_S and superconducting gap at absolute zero Δ_0 . The barrier resistance ζ is fixed at 7 ensuring the validity

of weak proximity regime. Temperature and junction width are $T = 0.05T_c$ and $W = 10\xi_S$. We use units such that $\hbar = k_B = 1$.

Figure 2 illustrates the response of the critical Josephson current in a planar junction to an external magnetic field as shown schematically in Fig. 1 A). Various parameter values have been considered in order to make our analysis as general as possible. To do so, we have considered three scenarios where the superconducting leads have different sizes (first row) and where they have equal sizes with a large (second row) and small (third row) separation distance. Specifically, the third row is relevant with regard to the experiment in Ref. 11 where the size of the electrodes far exceeds the separation distance. As seen, in this case the interference pattern exhibits a local minimum at $\Phi = 0$ rather than a maximum as in the Fraunhofer case, which is fully consistent with the experimental results in Ref. 11. Whereas it was speculated that this minimum might be attributed to a shift in the entire interference curve due to a finite sample magnetization in Ref. 11, it is obvious that this is not the case here since the sandwiched strip is not ferromagnetic. Moreover, such a shift would make the current vs. flux curve manifestly asymmetric (see *e.g.* Ref. 20), in contrast to the experimental results of Ref. 11 where the central minimum is flanked by two large peaks, similar to our results. Based on this, it seems reasonable to explain the deviation from the standard Fraunhofer pattern as a result originating from the combination of a planar geometry with the size and separation distance of the superconducting electrodes. The latter fact is seen by considering the second row of Fig. 2 where the separation distance is large compared to the superconductors: a Fraunhofer-like pattern emerges, although the decay becomes more monotonic as the thickness d of the normal strip increases. Even columns in both Figs. 2 and 3 show the pair potential where the superconducting phase difference is zero $\varphi = 0$ and external magnetic flux is set to $\Phi = 4\Phi_0$. As seen, the predicted proximity vortices in Refs. 4 and 10 vanish for the planar junction geometry. However, as

it will be discussed further below, they reappear in the specific case of a stacked geometry (Fig. 1 B).

It is instructive to contrast these results with the geometry of Fig. 1 B) where the two superconducting leads are connected to the normal strip at opposite edges. This is resemblant to the experimentally often used stacked geometry. The order of frames (critical current and corresponding pair potential spatial map) are identical to those in Fig. 3 and various lead sizes and locations are investigated. It is seen that the location and size of both terminals are vital in terms of determining how the critical current responds to the external flux. For instance, our results reveal that only in specific case where the width of the leads' are sufficiently large and connected to opposite edges precisely in front of each other does one recover a proximity-induced vortex pattern along with the Fraunhofer curve *i.e.* $I(\varphi, \Phi) \propto \Phi^{-1} \sin \Phi \sin \varphi$ which is a special case corresponding to the scenario of Ref. 4. The results for the other scenarios in Fig. 3 also show good consistency with previous experimental observations⁵.

It is worth examining the characteristic length scales and thus the radius of the current circulation in Fig. 4. To illustrate this, we consider for concreteness the simplest case of a wide S/N/S junction subject a perpendicular magnetic field (to see more details, see Ref. 4). In this particular case, the current density is given by $\mathbf{J}_x(\vec{R}, \varphi) = J_{0x} \sin(\varphi - 2\frac{\pi\Phi}{\Phi_0 W} y)$. As seen, the characteristic length scale L_c over which the current density changes upon moving along the y axis is $L_c \sim \Phi_0 W / \Phi$. Thus, for magnetic fields corresponding to several flux quanta L_c can be smaller than the junction size. With increasing external magnetic flux Φ , the current density flow shown in Fig. 4 takes on smaller radii. Instead, when decreasing the external flux $\Phi \rightarrow 0$, $L_c \rightarrow \infty$ which means there exists no current circulation in the system. In other words, the current density spatial map of the system is uniform in the absence of any external magnetic flux.

Having unveiled the origin of the anomalous inverted Fraunhofer response, we now turn to the second main result of this paper: the possibility to generate a φ -junction in an SNS system with an applied magnetic field. In Fig. 4, we provide the CPR in addition to a spatial map of the current-flow in the normal strip for three represented geometries. In *i*) the leads are connected opposite to each other, in *ii*) they are connected antisymmetrically, whereas in *iii*) they are connected symmetrically in a planar geometry similar to Ref. 11. It is clear that the CPR remains sinusoidal as a function of the superconducting phase-difference φ in both *i*) and *ii*) independent on the applied flux. However, case *iii*) is qualitatively different. The generic form of the CPR is now revealed as:

$$I(\varphi, \Phi) = I_0(\Phi) \sin(\varphi + \Theta(\Phi)) \quad (6)$$

in which $I_0(\Phi)$ and $\Theta(\Phi)$ are geometry-dependent functions of external magnetic flux as seen in Fig. 4. In fact, Eq. (6) holds for all situations considered in Fig. 2 where we have demonstrated the CPR is never purely sinusoidal. The standard sinusoidal CPR is recovered only for symmetric situations relative the induced orbital motion by the external magnetic field, see Fig. 1 C). This observation has a highly interesting consequence: the anomalous magnetic flux-coupled

CPR ensures that the ground-state of the system may be tuned so that the equilibrium phase difference differs from the conventional 0 or π solutions. Instead, a so-called φ -junction may be realized where the ground-state phase difference φ is tunable via the external flux. We therefor arrive at a ground-state with Josephson energy E_J which can be controlled by adjusting the applied external magnetic field. The idea of a φ -junction via a superconducting phase difference shift has been considered previously⁷ in the context of a non-centrosymmetric normal layer with a Rashba spin-orbit interaction. However, in our setup the external flux is a well-controlled parameter which allows for easy tuning of the ground-state, as opposed to controlling a spin-orbit interaction parameter. Moreover, our finding is different from Ref. 8 where two magnetic junctions, one in 0-state and the other in π -state with different lengths, are connected in parallel and consequently generate an extra cosinusoidal term in addition to negative second harmonic.

What is then the physical origin of this anomalous CPR? The answer to this question may be obtained by investigating the current density flow under the influence of an external magnetic field inside the normal strip, as seen in Fig. 4. For zero phase difference $\varphi = 0$, the external magnetic field induces a current flow where the orbital paths taken by the quasiparticles move with the same flux in and out of the superconducting regions, in effect no net current flow, *only in special geometrical configurations*. For instance, both in *i*) and *ii*) the current flow between the superconductors in any part of the normal region is seen to have an antisymmetric, and thus cancelling, contribution in a different part of the normal strip at zero phase difference $\varphi = 0$. In contrast, this is no longer the case in setup *iii*): there is a net flow of current induced by the orbital response due to the magnetic flux, even at $\varphi = 0$. To elucidate this clearly in the current-flow, one would have to consider the amplitude of the local current as well, but the supercurrent-phase curves nevertheless demonstrate that this interpretation is correct. In essence, this is a geometry-dependent effect since it relies on the positioning of the leads relative the induced current-flow via the applied field. Thus, it gives rise to the unique possibility to alter the standard CPR so that the ground-state of system can be adjusted by tuning the external flux.

To conclude, we have studied the Josephson critical current and its response to an external magnetic flux in experimentally feasible nonaligned junctions. Specifically, a planar geometry similar to a recent experiment¹¹ is considered and it is demonstrated that the observed suppression at zero flux may stem from the junction geometry rather than any intrinsic magnetization. Moreover, it is shown that a highly unusual supercurrent-phase difference-shift occurs inevitably in a class of nonaligned junctions due to an external magnetic flux. Its precise form is sensitive to the size and location of the superconducting leads. Consequently, this offers a route to a tunable junction ground-state. The physical origin of this effect is traced back to the induced current density flow due to the presence of an external field relative the position of the superconducting leads. As an interesting consequence, this type of Josephson junctions constitute an attainable way of realiz-

ing the so-called φ -junction experimentally.

We appreciate G. Sewell for his valuable instructions in the numerical parts of this work. We also thank F. S. Bergeret, E.

Goldobin, J. W. A. Robinson, V.V. Ryazanov and N. Birge for useful discussions/comments as well as K. Halterman for his generosity regarding compiler source.

-
- * Electronic address: phymalidoust@gmail.com
 † Electronic address: jacob.linder@ntnu.no
- ¹ B.D. Josephson, *Rev. Mod. Phys.* **36**, 216 (1964).
 - ² J.M. Rowell, *Phys. Rev. Lett.* **11**, 200 (1963); J. Clarke, *Proc. R. Soc. A* **308**, 447 (1969); S. Nagata, H. C. Yang, and D. K. Finnemore, *Phys. Rev. B* **25**, 6012 (1982); H. C. Yang and D. K. Finnemore, *Phys. Rev. B* **30**, 1260 (1984).
 - ³ J. P. Heida, B. J. van Wees, T. M. Klapwijk, and G. Borghs, *Phys. Rev. B* **57**, 5618 (1998); U. Ledermann, A. L. Fauchre, and G. Blatter, *Phys. Rev. B* **59**, 9027 (1999).
 - ⁴ J. C. Cuevas, and F. S. Bergeret, *Phys. Rev. Lett.* **99**, 217002 (2007); F. S. Bergeret, and J. C. Cuevas, *J Low Temp Phys* **153**, 304 (2008).
 - ⁵ L. Angers, F. Chiodi, G. Montambaux, M. Ferrier, S. Gueron, H. Bouchiat, and J. C. Cuevas, *Phys. Rev. B* **77**, 165408 (2008).
 - ⁶ A. Buzdin, and A. E. Koshelev, *Phys. Rev. B* **67**, 220504(R) (2003).
 - ⁷ A. Buzdin, *Phys. Rev. Lett.* **101**, 107005 (2008).
 - ⁸ E. Goldobin, D. Koelle, R. Kleiner, and R. G. Mints, *Phys. Rev. Lett.* **107**, 227001 (2011).
 - ⁹ L. N. Bulaevskii *et al.*, *JETP Lett.* **25**, 290 (1977); A. I Buzdin *et al.*, *JETP Lett.* **35**, 178 (1982).
 - ¹⁰ M. Alidoust, G. Sewell, and J. Linder, *Phys. Rev. Lett.* **108**, 037001 (2012).
 - ¹¹ R. S. Keizer, S. T. B. Goennenwein, T. M. Klapwijk, G. Miao, G. Xiao, and A. Gupta, *Nature* **439**, 825 (2006).
 - ¹² T. S. Khaire, W. P. Pratt, Jr., and N. O. Birge, *Phys. Rev. B* **79**, 094523 (2009); M. A. Khasawneh, W. P. Pratt, Jr., and N. O. Birge, *Phys. Rev. B* **80**, 020506(R) (2009); Y. Wang, W. P. Pratt, Jr., and N. O. Birge, *Phys. Rev. B* **85**, 214522 (2012).
 - ¹³ G. Mohammadkhani, M. Zareyan, and Ya. M. Blanter, *Phys. Rev. B* **77**, 014520 (2008); G. Mohammadkhani, Ph.D. thesis, Institute for Advanced Studies in Basic Sciences, Zanjan, Iran (2008).
 - ¹⁴ H. Sickinger, A. Lipman, M. Weides, R. G. Mints, H. Kohlstedt, D. Koelle, R. Kleiner, and E. Goldobin, *Phys. Rev. Lett.* **77**, 014520 (2008).
 - ¹⁵ K. D. Usadel, *Phys. Rev. Lett.* **25**, 507 (1970); A. I. Larkin and Y. N. Ovchinnikov, in *Nonequilibrium Superconductivity*, edited by D. Langenberg and A. Larkin (Elsevier, Amsterdam, 1986), P. 493.
 - ¹⁶ J. P. Morten, M.Sc. thesis, Norwegian University of Science and Technology (2003).
 - ¹⁷ M. S. Crosser, J. Huang, F. Pierre, P. Virtanen, T. T. Heikkila, F. K. Wilhelm, and N. O. Birge, *Phys. Rev. B* **77**, 014528 (2008).
 - ¹⁸ A. V. Zaitsev, *Zh. Eksp. Teor. Fiz.* **86**, 1742 (1984) (*Sov. Phys. JETP* **59**, 1015 (1984)); M. Y. Kupriyanov *et al.*, *Sov. Phys. JETP* **67**, 1163 (1988).
 - ¹⁹ G. Sewell, *The Numerical Solution of Ordinary and Partial Differential Equations, second edition*, John Wiley & Sons, (2005); G. Sewell, *Advances in Engineering Software* **41**, Iss. 5, 748-753 (2010).
 - ²⁰ J. W. A. Robinson, J. D. S. Witt, and M. G. Blamire, *Science* **329**, 5987 (2010); M. Alidoust, J. Linder, G. Rashedi, T. Yokoyama, and A. Sudbø, *Phys. Rev. B* **81**, 014512 (2010); M. Alidoust, and J. Linder, *Phys. Rev. B* **82**, 224504 (2010); G. B. Halasz, M. G. Blamire, and J. W. A. Robinson, *Phys. Rev. B* **84**, 024517 (2011); C. Wu, O. T. Valls, and K. Halterman, *Phys. Rev. Lett.* **108**, 117005 (2012); C. Wu, O. T. Valls, and K. Halterman, *Phys. Rev. B* **86**, 184517 (2012).
 - ²¹ Yu. S. Barash, *Euro Phys. Lett.* **91**, 37001 (2010); *Phys. Rev. B* **85**, 100503(R) (2012); *Phys. Rev. B* **86**, 144502 (2012).
 - ²² V. Barzykin, and A. M. Zagoskin, *Superlattices and Microstructures*, Vol. 25, No. 5/6, P. 797-807, 1999.
 - ²³ S.V. Bakurskiy, N.V. Klenov, T.Yu. Karminskaya, M.Yu. Kupriyanov, and A.A. Golubov, *Supercond. Sci. Technol.* **26**, 015005 (2013).